MSP Dynamics and Retraction in Nematode Sperm

Charles W. Wolgemuth

Department of Cell Biology, University of Connecticut Health Center, Farmington, CT 06030-3505

Abstract. Most eukaryotic cells can crawl over surfaces. In general, this motility requires three distinct actions: polymerization at the leading edge, adhesion to the substrate, and retraction at the rear. Recent *in vitro* experiments with extracts from spermatozoa from the nematode *Ascaris suum* suggest that retraction forces are generated by depolymerization of the Major Sperm Protein (MSP) cytoskeleton. Combining polymer entropy with a simple kinetic model for disassembly I propose a model for disassembly-induced retraction that fit the *in vitro* experimental data. This model explains the mechanism by which deconstruction of the cytoskeleton produces the force necessary to pull the cell body forward and suggest further experiments that can test the validity of the model.

Keywords: MSP; cell motility; gel; major sperm protein; mathematical model.
PACS: 87.17.Jj**,** 82.33.Ln, 82.35.Pq, 82.35.Rs, 83.10.Ff, 83.80.Kn

INTRODUCTION

Imagine that you are a single cell . . . and you're hungry. You have two options. The first is that you can stay stationary, remain in place, and wait for food to come to you. By far, this method is the easiest: it requires no energy output. However, as you may guess, it is risky. If food does not come, you will die. On the other hand, you can figure out how to move and go in search of food. This method is harder but more productive. You, the cell, must somehow figure out how to exert force on your environment in such a way that you can produce and maintain directed motion. It is not surprising that many cells have chosen this route. The expense of energy is a small price to pay to stay alive. It is also not surprising that cells have figured out many different methods for achieving motility.

As with organisms at our scale, cells live in one of two environments. They are either immersed in a fluid or they live at a surface (here I loosely consider surrounding cells, such as in tissue, a surface as well). Swimming and flying are the types of motility possible for beings that are immersed. At the cellular scale, the predominant fluid is water. As the density of a cell is comparable to that of water, producing lift force is not an issue, and, indeed, cells are not known to fly. Swimming, however, is

very common. As has been discussed in a number of the talks here at this symposium, many cells swim by waiving or rotating filamentary objects or composites of filamentary objects. The drag force that the fluid exerts back on these undulating cilia or flagella produces the thrust that pushes the cell forward.

When in contact with a surface, a cell must somehow leverage friction to enable motility, just as we must to walk. Both eukaryotic cells and prokaryotic cells have figured out how to do this, though with quite different mechanisms. In this talk I will focus on the method employed by eukaryotic cells, which is generically called crawling. In general, this motility requires three distinct actions: polymerization at the leading edge, adhesion to the substrate, and retraction at the rear (**Figure 1**)[1-3]. A more detailed description of the model that I will discuss is presented elsewhere [4].

One of the main cytoskeletal components of eukaryotic cells is a cross-linked polymer network composed of actin filaments. Polymerization and addition of new actin filaments at the leading edge of the cell drives extension through either a polymerization ratchet mechanism [5-6] or swelling [7-9]. Transmembrane proteins, such as integrins, anchor cells to the substrate [10-12]. The mechanism by which force is generated to drive translocation of the cell body is still debated. Originally, this force was attributed to an actomyosin system similar to muscle [13]. However, Myosin II-null *Dictyostelium* cells are still capable of translocation [14-15]. Mogilner and Oster suggested that the depolymerization of an actin meshwork could generate a contractile force to pull up the cell rear [16]. Here we present a more detailed analysis of contractile force generation in a cell that lacks cytoskeletal protein motors. This problem has been addressed previously by finite element modeling [17] and continuum modeling [18-20]; the treatment here offers a microscopic explanation for the *in vitro* experiments on MSP force production [21] and its implications for nematode sperm locomotion.

MSP AND NEMATODE SPERM CRAWLING

Spermatozoa from nematodes, such as *Ascaris suum*, exhibit crawling motility strikingly similar to those of other crawling cells. Although they show all three characteristics of crawling, they do not possess an actin cytoskeleton. Rather, the nematode sperm utilizes a gel of an unrelated polymer, Major Sperm Protein (MSP). As in actin-based cells, polymerization of MSP at the leading edge of the lamellipod produces the force necessary to push out the front of the cell [22]. Unlike actin, MSP forms non-polar filaments [23], and molecular motors have not been identified. These results strongly suggest that the dynamics of the MSP network is responsible for both protrusive and retraction forces in crawling sperm cells. Recent *in vitro* experiments using cellular extracts from *A. suum* spermatozoa implicate disassembly of the MSP network as the force generating mechanism driving translocation of the cell body [21]. In these experiments, vesicles made from the membrane of *A. suum* sperm in the presence of sperm cytosol induce polymerization of a ‘comet tail’ cylinder of MSP that pushes the vesicle [22], similar to the motion of ActA coated beads in the presence of actin [24]. Retraction forces could be induced in the MSP gel by addition of *Yersinia enterocolytica* tyrosine phosphatase (YOP) to the cell-free extract of sperm

(S100) in marked contrast to the behavior of the comet tails in buffer solution which only showed slight retraction [21].

In nematode sperm, MSP forms a network of interconnected charged filaments surrounded by cytosolic fluid, that constitutes a polyelectrolyte gel. This gel exhibits two coexisting forms: a distributed gel consisting of MSP filaments, and condensed regions of filaments (also called ‘fiber complexes’, ‘bundles’ or 'ribs') that span the lamellipod from the leading edge to the cell body. The arrangement of the filaments throughout the lamelipod appears to be mostly isotropic; however, images taken by electron microscopy show a bottle brush structure in the fiber complexes [25], suggesting that the filaments may be more ordered in these regions. The *in vitro* experiments on vesicles suggest that solation of this MSP gel induces contractile forces that pull the cell body forward.

THE DEPOLYMERIZATION WINCH

The MSP cytoskeleton is a gel: a crosslinked polymer network immersed in fluid. The volume of such gels is determined by the equilibrium between four forces [20,26]: (i) the entropic tendency for the gel filaments to diffuse outwards, (ii) the ‘counterion pressure’ that tends to inflate the gel, (iii) the entropic elasticity of the gel filaments that tends to resist expansion, and (iv) the attractive interactions between the filaments that also tend to hold the gel together. In gels, crosslinking of the filaments increases

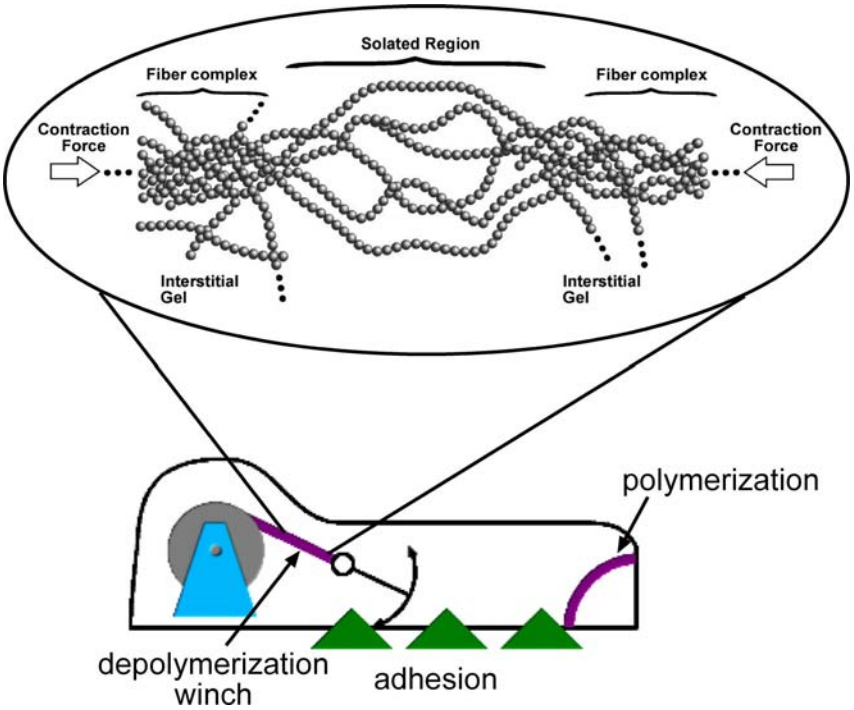

FIGURE 1. Schematic of the model for cell crawling. Polymerization of the leading edge pushes out the front of the cell. Adhesion to the substrate provides traction. We propose that depolymerization of the cytoskeleton produces the force necessary to haul the cell body forward.

the rigidity of the overall structure and locks out entropic degrees of freedom. *Solation* involves breaking chains. When the structure solates, the rigidity of the structure decreases and the gain in filament entropic freedom drives retraction of the network (**Figure 1**). The energy sources for contractile work are the free energies of polymerization and crosslinking.

To quantitate this model, we denote by M_p the total mass of polymer in the gel. This mass can be related to the volume, V, of the gel through the volume fraction, ϕ, the ratio of polymer volume to the total mass of the gel (polymer plus solvent). $M_p = \rho_p \phi V$, where ρ_p is the density of a monomer of the polymer. Depolymerization of the polymer decreases the mass, but also can affect ϕ. Whether the gel contracts or not, depends on the ratio of these two effects.

Solation of the gel phase proceeds in two steps. First, chains are severed from the bulk gel creating chains with free ends. Second, the free ends depolymerize into monomers. Therefore, the polymer network contains two kinds of chains: those where both ends terminate in a crosslink, and those where one end is free. Let M_f be the mass of polymer in the free chains and M_c the mass in connected chains. The simplest model assumes that connected chains get broken and are transformed into free chains, which then depolymerize. The kinetics for this model are

$$\begin{aligned} \frac{dM_c}{dt} &= -k_c M_c \\ \frac{dM_f}{dt} &= k_c M_c - k_f M_f \end{aligned} \tag{1}$$

with rate constants k_c and k_f. The total mass is $M_p = M_c + M_f$.

As mentioned above, solation increases the entropic freedom of the polymer in the gel and can lead to contraction. EM images show MSP filaments that are often bent at lengths of tens of nanometers, suggesting that this length is comparable to the persistence length of MSP [17]. Therefore, it is reasonable to treat the MSP filaments composing the cytoskeletal meshwork as flexible. Using a Flory-Huggins free energy [26] and assuming an isotropic and homogeneous gel, the stress, σ, is a function solely of the volume fraction:

$$\left(\frac{V_m}{k_B T}\right)\sigma_{ij} = \left(\underbrace{-\ln(1-\phi)-\phi}_{\text{mixing}} - \underbrace{\chi\phi^2}_{\substack{\text{polymer}\\ \text{interaction}}} + \underbrace{\frac{1}{N_e}\left(\frac{1}{2}\phi - \phi_0^{2/3}\phi^{1/3}\right)}_{\text{elasticity}} - \underbrace{2N_A V_m (C_{ion} - C_b)}_{\substack{\text{counterion}\\ \text{pressure}}} \right)\delta_{ij} \tag{2}$$

Here N_A is Avogadro's number, V_m is the volume of a monomer, k_B is Boltzmann's constant, and T is the temperature, and δ_{ij} is the identity matrix. χ is the Flory parameter which measures the interaction energy between polymer chains [26]. Solation of the gel breaks crosslinks, which changes effective number of monomers between crosslinks, N_e. As crosslinks are destroyed, N_e should increase. I assume a simple kinetics with a rate proportional to the rate that connected chains are broken,

$$\frac{dN_e}{dt} = \beta k_c M_c \tag{3}$$

where β is a constant

To compare the model derived above with the experiments in [21], length and optical density (OD) are converted to MSP mass and volume fraction using $M_p = \rho_p \phi V$ and Beer's law to relate the optical density to the volume fraction. The results are shown in **Figure 2**a, b. Both the mass and the volume fraction decrease as a function of time; however, the mass decreases faster than the volume fraction which requires an overall contraction of the MSP network. Using the mass vs. time plot, we fit the parameters k_f and k_c in KPM buffer and in S100 supplemented with YOP. We find good fits with a value of $k_f = 0.5$ min^{-1} and $k_c = 0.05$ min^{-1} in KPM buffer and $k_c = 0.14$ min^{-1} in S100 + YOP (**Figure 2**a,b). The depolymerization rates for MSP comet tails have not been measured; however, the value found for k_f is roughly comparable to the depolymerization rate for actin measured in crude extracts and *in vivo* [27,28].

Next we modeled the change in volume fraction, ϕ, with time using the determined values for k_c and the gel stress model for the solation of the MSP network. We find good agreement between the model and the data (**Figure 2**b). As shown in the figure, the volume fraction of the MSP gel decreases during the first 10 minutes and then tends to flatten out for both solution chemistries. In S100 supplemented with YOP, this decrease is more rapid than in KPM buffer. To compare the values calculated in this manner with the original data, we plot the change in length and optical density using the model. **Figure 2**c-d show that both solation models capture the disassembly and retraction of the MSP gel.

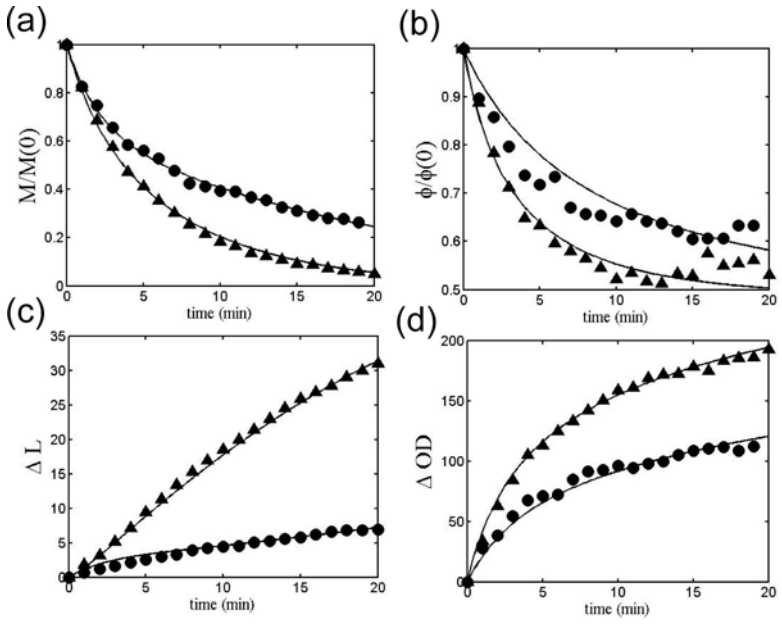

FIGURE 2. Model fits to data taken from [21]. (a) MSP polymer mass vs. time. (b) MSP volume fraction vs. time. (c) Cumulative loss in length of an MSP fiber vs. time. (d) Cumulative loss in optical density vs. time. (a-d) Circles (KPM buffer media) and triangles (s100 and YOP media) represent a replotting of the data from [21]. (a) Solid line is a fit to the mass kinetic model. (b-d) Solid lines are a fits using the gel retraction model.

The experiments that have been done so far show that disassembly can produce retraction in MSP fibers associated with vesicles. However, these experiments do not show directly that this retraction can produce sufficient force to pull the cell body forward during crawling. The model suggests an experiment that can test the force production by disassembly of the MSP network. [21] observed that a bead could be attached to the MSP fiber and pulled along with the retracting fiber. If a bead is adhered to each end of the MSP fiber, the force required to prevent retraction can be measured using micromanipulation techniques such as flexible handles [29]. If we assume that under these conditions, the volume of the MSP fiber stays fixed, then $\phi = M/\rho_m V$. The force required to hold the ends is just the magnitude of the elastic stress times the cross-sectional area of the MSP tail.

Figure 3b shows that the maximum force on the comet tail produced by fiber depolymerization does not depend strongly on the presence of YOP. Both situations produce a maximum force ~ 30 nN. This force is comparable to the experimentally measured force required to halt crawling in keratocytes [30]. However, since a crawling cell traverses a cell length per minute, the physiological translocation force per bundle is more reasonably estimated by the force generated during the first minute. This force is found to be 5 nN in KPM buffer and 15 nN for S100 + YOP. Interestingly, the model predicts a slower rise for the force produced in the presence of YOP where the network is being disassembled faster. This result is somewhat counterintuitive since it seems that faster disassembly should lead to faster force production. However, the elastic strength of the network depends strongly on the crosslink density, whereas the stress depends strongly on the volume fraction, ϕ. In KPM buffer, the MSP mass that is contained in the free chains quickly depolymerizes, but crosslinks and connected chains stay intact. Therefore, the elasticity of the network remains strong, while entropic pressure from the free chains is removed driving network contraction. When YOP is added, crosslinks are broken more quickly. Therefore, the elasticity of the network decreases and free chain polymer is removed from the system at comparable rates; therefore, force production is slower. At longer times, the force decreases as the elasticity in the network is degraded.

This force dynamics may play a role in nematode sperm translocation. As the cell crawls, new polymer is added at the leading surface and old polymer gets progressively closer to the rear of the cell where disassembly induces the retraction necessary to pull the cell body forward. At the front of the cell, adhesion to the substrate is strong. Therefore, applying large forces at the leading edge are ineffective—or even counterproductive—if the force is large enough to break the adhesion to the substratum. Slower force production in the presence of YOP shifts the location of strong retraction towards the rear of the cell where it is most effective in pulling the cell body forwards.

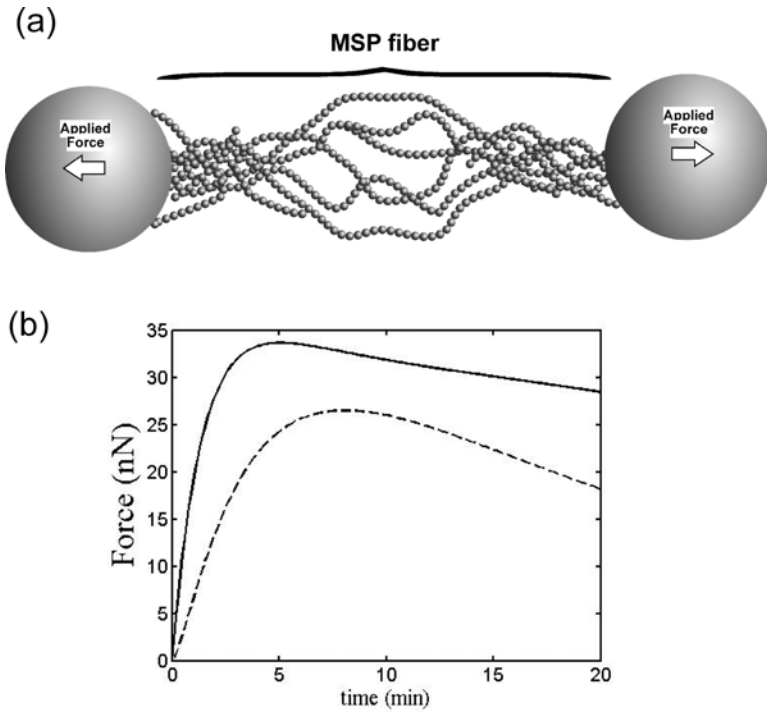

FIGURE 3. (a) Schematic of the proposed experiment. (b) Plot of force vs. time derived from the model when both ends of the MSP fiber are held fixed. The solid line shows the result for the MSP fiber in KPM buffer. The dashed line is the result for the MSP fiber in cell-free extract and YOP.

ACKNOWLEDGMENTS

The author thanks G. Oster, T. Roberts, O. Vanderlinde, and L. Miao for their contributions to this project.

REFERENCES

1. Abercrombie, M., *Proc. Roy. Soc. Lond. B* **207**, 129-147 (1980).
2. Lauffenburger, D.A., and Horwitz, A.F., *Cell* **84**, 359-369 (1996).
3. Mitchison, T.J., and Cramer, L.P., *Cell* **84**, 371-379 (1996).
4. Wolgemuth, C.W., Miao, L., Vanderlinde, O., Roberts, T., and Oster, G., (preprint).
5. Mogilner, A., and Oster, G., *Biophy. J.* **84**, 1591-1605 (2003).
6. Peskin, C., Odell, G., and Oster, G., *Biophys. J.* **65**, 316-324 (1993).
7. Herant, M., Marganski, W.A., and Dembo, M., *Biophys. J.* **84**, 3389-3413 (2003).
8. Oster, G., and Perelson, A., "The physics of cell motility," in *Cell Behavior: Shape, Adhesion and Motility*, edited by J. Heaysman CM, F. Watt, Cambridge, England: The Company Of Biologists Ltd., 1988, p. 35-54.
9. Oster, G., and Perelson, A., "Cell protrusions," in *Frontiers in Mathematical Biology*, edited by S. Levin, Berlin: Springer-Verlag, 1994, p. 53-78.
10. Gaudet, C., Marganski, W.A., Kim, S., Brown, C.T., Gunderia, V., Dembo, M., and Wong, J.Y., *Biophys. J.*, **85**, 3329-3335 (2003).
11. Koo, L.Y., Irvine, D.J., Mayes, A.M., Lauffenburger, D.A., and Griffith, L.G., *J. Cell Sci.*, **115**, 1423-1433 (2002).
12. Rahman, A., Tseng, Y., and Wirtz, D., *Biochem. Biophys. Res. Commun.*, **296**, 771-778 (2002).

13. Huxley, H.E., *Nature*, **243**, 445-449 (1973).
14. DeLozanne, A., and Spudich, J.A., *Science*, **236**, 1086-1091 (1987).
15. Knecht, D.A., and Loomis, W.F., *Science*, **236**, 1081-1086 (1987).
16. Mogilner, A., and Oster, G., *Euro. Biophys. J.*, **25**, 47-53 (1996).
17. Bottino, D., Mogilner, A., Stewart, M., Roberts, T., and Oster, G., *J. Cell Sci.*, **115**, 367-384 (2001).
18. Joanny, J.F., Julicher, F., and Prost, J., *Phys. Rev. Lett*., **90**, Art. No. 168102 (2003).
19. Mogilner, A., and Verzei, D.W., *J. Stat. Phys*., **110**, 1169-1189 (2003).
20. Wolgemuth, C.W., Mogilner, A., and Oster, G., *Eur. Biophys. J*., **33**, 146-158 (2004).
21. Miao, L., Vanderlinde, O., Stewart, M., and Roberts, T.M., *Science*, **302**, 1405-1407 (2003).
22. Italiano, J.J., Roberts, T.M., Stewart, M., and Fontana, C.A., *Cell*, **84**, 105-114 (1996).
23. Bullock, T.L., Roberts, T.M., and Stewart, M., *J. Mol. Biol*., **263**, 284-296 (1996).
24. Cameron, L.A., Footer, M.J., Oudenaarden, A.V., and Theriot, J.A., *Proc. Natl. Acad. Sci. USA*, **96**, 4908-4913 (1999).
25. Sepsenwol, S., Ris, H., and Roberts, T.M., *J. Cell Biol*., **108**, 55-66 (1989).
26. Flory, P.J., *Principles of Polymer Chemistry*, Ithaca, NY: Cornell Univeristy Press (1953).
27. Theriot, J.A., Rosenblatt, J., Portnoy, D.A., Goldshmidt-Clermont, P.J., and Mitchison, T.J., *Cell*, **76**, 505-517 (1994).
28. Watanabe, N., and Mitchison, T.J., *Science*, **295**, 1083-1085 (2002).
29. Marcy, Y., Prost, J., Carlier, M.-F., and Sykes, C., *Proc. Natl. Acad. Sci. USA*, **101**, 5992-5997 (2004).
30. Oliver, T., Lee, J., and Jacobson, K., *Semin. Cell Biol*., **5**, 139-147 (1994).